CONF-831111--8

UCRL--89602

DE83 017618

COMPUTER IMPLEMENTATION, ACCURACY, AND TIMING OF RADIATION VIEW-FACTOR ALGORITHMS

Arthur B. Shapiro

This paper was prepared for submittal to the
1983 ASME Winter Meeting, Boston, MA.
November 14-18, 1983

MASTER

July, 1983

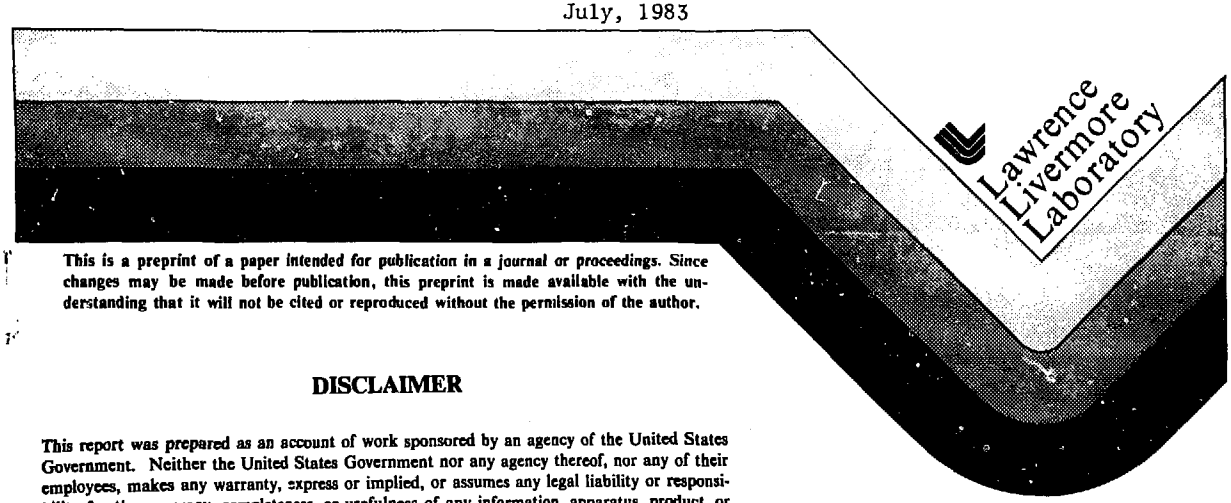

DISCLAIMER

COMPUTER IMPLEMENTATION, ACCURACY AND TIMING OF RADIATION VIEW-FACTOR ALGORITHMS

Arthur B. Shapiro
University of California, Lawrence Livermore National Laboratory
Livermore, California 94550, U.S.A.

ABSTRACT

The three-dimensional finite-element thermal analysis of enclosure radiation problems requires the calculation of the geometric surface-to-surface radiation view factors. The view factors can be calculated by either area or line integration algorithms. This paper addresses the implementation, accuracy, and computational time involved in using these algorithms. Additionally, an algorithm to identify shadowing surfaces and methods to adjust the calculated view factors for increased accuracy are presented.

INTRODUCTION

At the Lawrence Livermore National Laboratory several projects require the three-dimensional finite element thermal analysis of problems involving conduction in a solid coupled with radiation in enclosures within the solid. An enclosure is defined by the discrete boundary surfaces of finite elements which surround the enclosure and define the solid object. Other objects, such as radiation shields, may be present within the enclosure. To calculate the radiation transport within the enclosure, the geometric surface to surface black body radiation view factors are required. Several computer codes (1-3) are available to calculate the view factor between two surfaces with the possibility of third surface shadowing. These codes use either area or line integration algorithms to calculate view factors without shadowing. In the presence of shadowing, all these codes use area integration algorithms with various techniques to account for the shadowing.

Extensive computations at LLNL in solving large two-dimensional enclosure radiation problems with 700 to 1000 participating segments revealed that up to three hours of computer time[1] were required to calculate view factors. The subsequent steady state thermal analysis using these view factors required under 20 minutes of computation time. The inaccuracies in the final results were attributable to inaccurate view factors between surfaces with third surface shadowing. As a result of this experience, before extending our analyses to three dimensions, the computational timing and accuracy of the various three-dimensional view factor algorithms needed to be quantified. This paper addresses the computer implementation, accuracy and computational time involved in using these algorithms. Additionally, an algorithm to identify shadowing surfaces and methods to adjust the calculated view factors for increased accuracy are presented.

VIEW FACTOR ALGORITHMS

The geometric black body radiation view factor between two surfaces, Fig. 1, is

$$F_{IJ} = \frac{1}{A_I} \int_{A_I} \int_{A_J} \frac{\cos\theta_I \cos\theta_J \, dA_I \, dA_J}{\pi r^2} \qquad (1)$$

If the two surfaces A_I and A_J are divided into n finite subsurfaces $A_i : i = 1,2,\ldots,n$ and $A_j : j=1,2,\ldots,n$, Eq. (1) may be approximated by

$$F_{IJ} \approx \frac{1}{A_I} \sum_{i=1}^{n} \sum_{j=1}^{n} \frac{\cos\theta_i \cos\theta_j A_i A_j}{\pi r_{ij}^2} \qquad (2)$$

The computational scheme, Eq. (2), is referred to as double area summation and is used in the computer codes (1-3) if shadowing exists.

The area integrals in Eq. (1) can be transformed to line integrals by using Stokes' theorem (5). The result is

[1] A CRAY-1 computer was used for all computations. The CRAY-1 has a 64 bit word length and an add time of 0.025 to 0.075 usec.

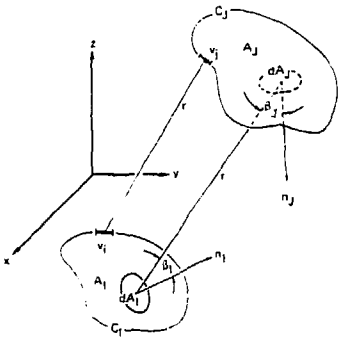

FIG. 1 THIS SKETCH ILLUSTRATES THE SYMBOLS USED IN EQS. (1) THROUGH (4) TO CALCULATE THE VIEW FACTOR F_{I-J}.

$$F_{IJ} = \frac{1}{2\pi A_I} \oint_{C_I} \oint_{C_J} (\ell n\, r\, dx_I\, dx_J + \ell n\, r\, dy_I\, dy_J + \ell n\, r\, dz_I\, dz_J) \tag{3}$$

If the two contours C_I and C_J are divided into n finite straight line segments $\hat{v}_i$: i=1,2,...,n and $\hat{v}_j$: j=1,2,...,n , Eq. (3) may be approximated by

$$F_{IJ} \simeq \frac{1}{2\pi A_I} \sum_{i=1}^{n} \sum_{j=1}^{n} \ell n\, r_{ij}\, \hat{v}_i \cdot \hat{v}_j \tag{4}$$

Mitalas and Stephenson (4) present a method by which one of the integrals in Eq. (3) can be integrated analytically. If the surfaces I and J are quadrilaterals, the result is

$$F_{IJ} = \frac{1}{2\pi A_I} \sum_{p=1}^{4} \sum_{q=1}^{4} \Phi(p,q) \oint_{C_p} [(T \cos\phi\, \ell n\, T + S \cos\theta\, \ell n\, S + U\omega - R)dv]_{p,q} \tag{5}$$

where S, T, U, ϕ, and ω are functions of v and

$$\Phi(p,q) = \ell_p \ell_q + m_p m_q + n_p n_q \tag{6}$$

The symbols are defined in Fig. 2. Dividing each of the four line segments C_p into n finite straight line segments $\hat{v}_j$: j=1,2,...,n, Eq. (5) may be approximated by

$$F_{IJ} \simeq \frac{1}{2\pi A_I} \sum_{p=1}^{4} \sum_{q=1}^{4} \Phi(p,q) \sum_{j=1}^{n} [(T \cos\phi\, \ell n\, T + S \cos\theta\, \ell n\, S + U\omega - R)\, |\hat{v}_j|]_{p,q} \tag{7}$$

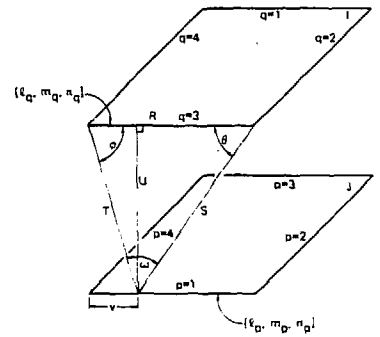

FIG. 2 THIS SKETCH ILLUSTRATES THE SYMBOLS USED IN MITALAS AND STEPHENSON'S CONTOUR INTEGRATION METHOD, EQS. (5) AND (6), TO CALCULATE THE VIEW FACTOR F_{I-J}.

The computational schemes represented by Eqs. (2), (4), and (7) will subsequently be referred to as the area integration method (AI), line integration method (LI), and the Mitalas and Stephenson method (MS), respectively. The surfaces between which view factors are being calculated are plane quadrilaterals. Methods LI and MS require a subdivision of the contour of the quadrilateral while method AI requires a subdivision of the surface area. Dividing each of the four line segments forming the quadrilateral into n divisions results in a total of 4n nodes around the contour and n^2 nodes for the surface area.

Operation counts for the three methods are:

AI Method	$114n^4 + 86n^2$
LI Method	$464n^2 + 24n$
MS Method	$864n + 288$

Timing studies, Fig. 3, show that the LI method is faster than the AI method for $n \geq 2$. Coding of the LI method results in FORTRAN DO - loops which are vectorized by the CRAY CFT (6) compiler. As a result of vectorization, the LI method having more operations is faster than the MS method for $n < 18$. Timing studies for the LI and MS methods are presented in Fig. 4.

The use of the numerical approximations for calculating the view factor, Eqs. (2), (4), and (7), assumes that the distance between the two surfaces is large compared to the differential approximates A_i, A_j and $\hat{v}_j$. As the distance between the two surfaces approaches the magnitude of A_i, A_j, and $\hat{v}_j$, the calculated view factor becomes increasingly inaccurate. This is shown in Fig. 5 where the separation distance between two directly opposed 1x1 squares is decreased from 10 to 1. The least accurate solution exists when the two surfaces share a common edge. To obtain a greater accuracy in the numerical calculations, the number of nodes, n, should be increased. Figures 6 and 7 show the percent error as a function of the number of nodes for directly opposed 1x1 squares and

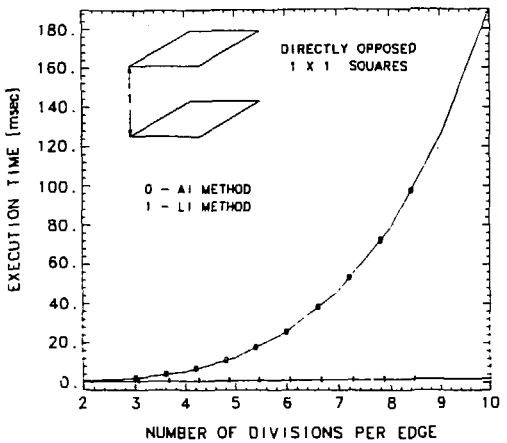

FIG. 3 AN OPERATION COUNT SHOWED THAT $114n^4 + 86n^2$ and $464n^2 + 24n$ OPERATIONS ARE REQUIRED FOR THE AI and LI METHODS, RESPECTIVELY. THE LI METHOD IS FASTER THAN THE AI METHOD FOR n>2.

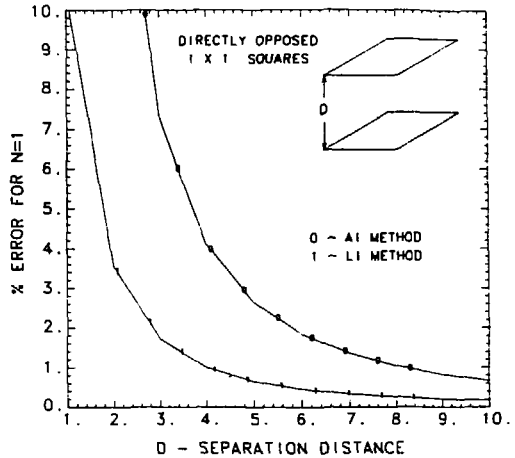

FIG. 5 THE USE OF THE NUMERICAL APPROXIMATIONS FOR CALCULATING THE VIEW FACTOR, EQS. (2), (4), AND (7), ASSUMES THAT THE DISTANCE BETWEEN THE TWO SURFACES IS LARGE COMPARED TO THE DIFFERENTIAL APPROXIMATES A_i , A_j , and v_j. AS THE DISTANCE BETWEEN THE TWO SURFACES APPROACHES THE MAGNITUDE OF A_i, A_j, AND v_j, THE CALCULATED VIEW FACTOR BECOMES INCREASINGLY INACCURATE.

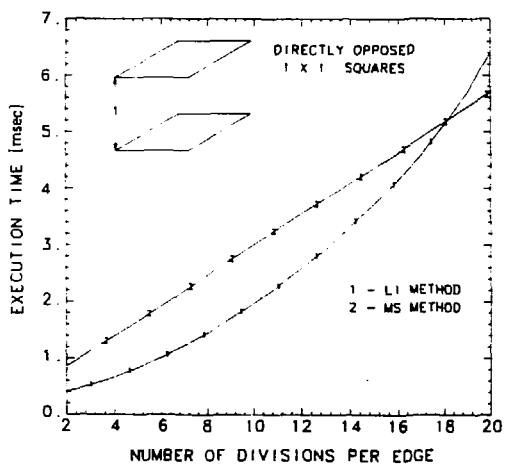

FIG. 4 AN OPERATION COUNT SHOWED THAT $464n^2 + 24n$ AND $864n + 288$ OPERATIONS ARE REQUIRED FOR THE LI AND MS METHODS, RESPECTIVELY. AS A RESULT OF VECTORIZATION OF THE LI METHOD BY THE CRAY COMPILER, THE LI METHOD HAVING MORE OPERATIONS IS FASTER THAN THE MS METHOD FOR n<18.

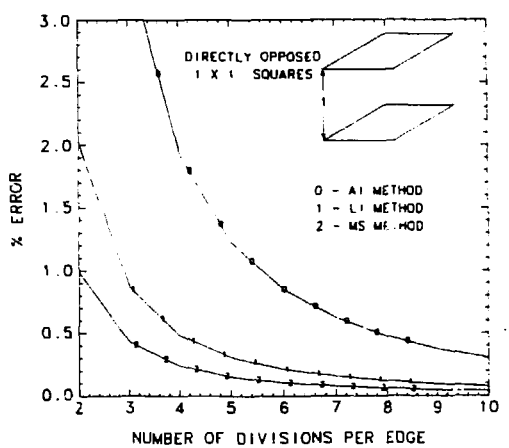

FIG. 6 THE LINE INTEGRATION METHODS, LI AND MS, ARE SIGNIFICANTLY MORE ACCURATE THAN THE AREA INTEGRATION METHOD AI. THE MS METHOD HAVING ONE OF ITS LINE INTEGRALS PERFORMED ANALYTICALLY IS MORE ACCURATE THAN THE LI METHOD.

perpendicular 1x1 squares, respectively. The line integration methods, LI and MS, are significantly more accurate than the area integration method AI. The MS method having one of its line integrals performed analytically is more accurate than the LI method. The AI method is so inaccurate when the two surfaces share a common edge, Fig. 7, that it should not be used.

In conclusion, the AI method should not be used. The LI method is less accurate but the execution time is faster than the MS method. Based on accuracy and execution time, Fig. 8, the LI method is superior to the MS method for n<7. For geometries other than directly opposed 1x1 squares with a separation distance of 1, the value of n for the break-even point is of course different.

SHADOWING AND OBSTRUCTIONS

Three types of shadowing may exist between two surfaces. There may be total self shadowing, partial self shadowing, and third surface shadowing. Total or partial self shadowing can be detected between two surfaces by looking at the angles θ_I and θ_J (Fig. 1). If $\cos\theta_I > 0$ and $\cos\theta_J > 0$, then the two surfaces can "see" each other. This is equivalent to verifying that

$$\hat{r}_{IJ} \cdot \hat{n}_I > 0$$
and (8)
$$\hat{r}_{JI} \cdot \hat{n}_J > 0$$

For plane quadrilaterals, it is necessary to verify these dot product inequalities for all vectors $\hat{r}$ connecting the four corner points between the two surfaces, a total of 16 $\hat{r}$. If Eqs. (8) are not satisfied for all $\hat{r}_{ij}$:i=1,2,3,4;j=1,2,3,4, then there is total self shadowing. If Eqs. (8) are satisfied for some $\hat{r}_{ij}$, then there is partial self shadowing.

Third surface shadowing can be detected by determining if a line connecting the centroids of the two surfaces for which a view factor is being calculated intersects other enclosure surfaces. The accuracy of this detection scheme can be improved if the lines connecting the corner points of the quadrilaterals are also checked for intersection with other enclosure surfaces. Unless those surfaces that can be shadowing surfaces are flagged on input to the computer code, all enclosure surfaces must be checked for each pair of surfaces for which a view factor is being calculated. This is a very time consuming operation.

The view factor can be calculated by the AI method, Eq. (2), when partial self shadowing or third surface shadowing exists. The two surfaces, Fig. 9, for which a view factor is being calculated are divided into finite subsurfaces. Contributions to the summation in Eq. (2) are not included for those subsurfaces in which the ray $\hat{r}_{ij}$ fails to satisfy Eqs. (8) or intersects a shadowing surface. For the configuration in Fig. 10, the view factor F_{IJ} approaches the analytical value of 0.115621 as the number of subsurfaces are increased.

The LI or MS methods can also be used to calculate the view factor between the AI subsurfaces. Again, a decision has to be made between accuracy and

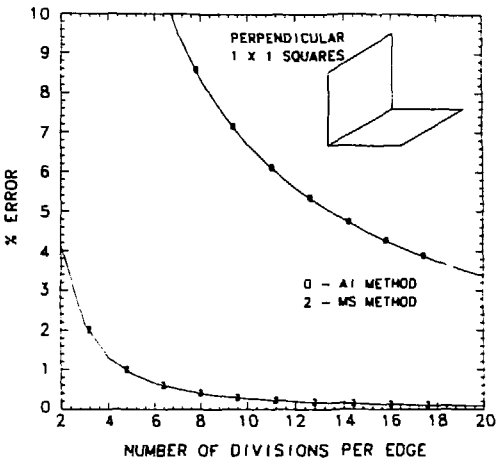

FIG. 7. THE LEAST ACCURATE NUMERICAL SOLUTION EXISTS WHEN THE TWO SURFACES SHARE A COMMON EDGE. THE AI METHOD IS SO INACCURATE THAT IT SHOULD NOT BE USED.

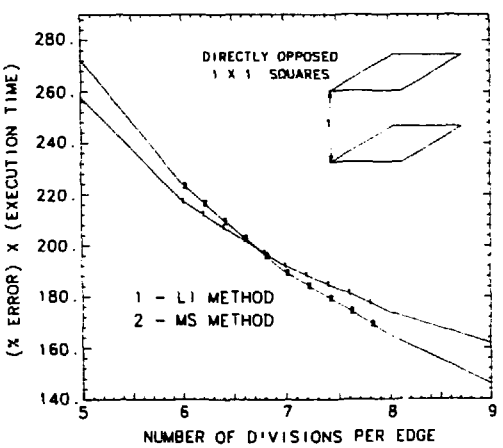

FIG. 8 BASED ON ACCURACY AND EXECUTION TIME, THE LI METHOD IS SUPERIOR TO THE MS METHOD FOR N<7.

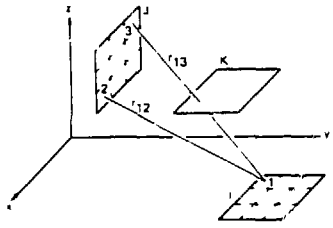

FIG. 9 THIS SKETCH ILLUSTRATES THIRD SURFACE SHADOWING. THE CONTRIBUTION TO THE SUMMATION IN EQ. (2) FOR SUBSURFACES 1-3 ARE NOT INCLUDED BECAUSE r_{13} INTERSECTS SURFACE K.

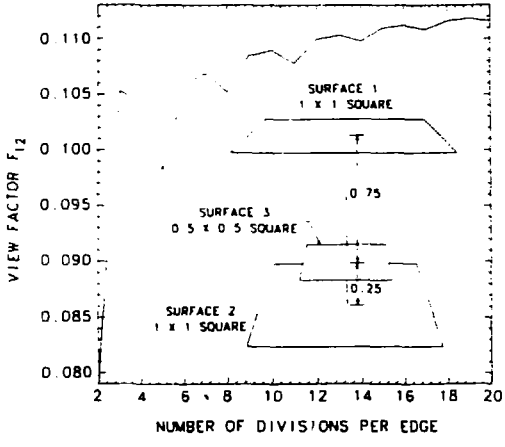

FIG. 10 SURFACE 3 SHADOWS THE VIEW BETEWEEN SURFACES 1 AND 2. THE VIEW FACTOR F_{12} APPROACHES THE ANALYTICAL VALUE OF 0.115621 AS THE NUMBER OF DIVISIONS ARE INCREASED.

computation time in selecting the best method. Since the view factor is being calculated between subsurfaces obtained by dividing an already small finite element mesh, the AI method may provide satisfactory results. Additionally, if the subsurfaces are not further subdivided (i.e. n=1 for the subsurface), the AI method is faster than LI or MS.

VIEW FACTOR ADJUSTMENT

The convergence of the AI method to the exact answer for problems with shadowing, Fig. 10, is not a smooth function of the number of nodes used for surface subdivision. A better approximation to the view factor with a savings in computer time can be calculated by a least squares curve fit and extrapolation to $n=\infty$ of the function $F_{IJ} = F_{IJ}(1/n)$.

A quadratic least squares curve fit and extrapolation was tried using F values for $n<10$. Completely erroneous results are obtained using F_{12} values (Fig. 10) at n=4,5 and 6. Selecting only monotonic F_{12} values, such as for n=4,6 and 7, a view factor of $F_{12}=0.118429$ (2.27% error) was calculated in 0.08 seconds.

At $n\geq 10$, where F_{12} is approaching a linear function in n, a linear least squares curve fit and extrapolation gave satisfactory results. A value of $F_{12}=0.113671$ (1.69% error) was calculated for the configuration of Fig. 10 using F_{12} values at n=10,11 and 12. The three view factor calculations, curve fit and extrapolation required 3.44 seconds of computer time. 61.5 seconds of computer time with n=30 are required to calculate the view factor with the same accuracy without a curve fit and extrapolation.

CONCLUSIONS

The geometric surface to surface black body radiation view factor can be numerically calculated by either area or line integration algorithms. The area integration method is so inaccurate that it should not be used when the two surfaces have an unshadowed view of each other. Computer implementation of the line integration method proposed by Sparrow (5) is vectorized by the CRAY compiler. As a result of vectorization, Sparrow's method having more operations is faster then the line integration method of Mitalas and Stephenson (4). However, the Mitalas and Stephenson method having one of its line integrals performed analytically is more accurate. Based both on accuracy and computer time, Sparrow's method is superior over the range of contour subdivisions typically used.

The area integration method should be used when partial self shadowing or third surface shadowing exists. The convergence of the area integration method to the exact answer is not a smooth function of the number of nodes used for surface subdivision. A linear least squares curve fit and extrapolation to $n=\infty$ of the function $F_{IJ} = F_{IJ}(1/n)$ results in a better approximation to the view factor with a savings in computer time.

ACKNOWLEDGEMENTS

This work was performed at the Lawrence Livermore National Laboratory under the Department of Mechanical Engineering, Methods Development Group, for the U.S. Department of Energy under contract number W-7405-Eng-48.

REFERENCES

1. R. L. Wong, "User's Manual for CNVUFAC - The General Dynamics Heat Transfer Radiation View Factor Program", University of California, Lawrence Livermore National Laboratory, UCID-17275 (1976).

2. E. F. Puccinelli, "View Factor Computer Program (Program VIEW) User's Manual", Goddard Space Flight Center, Greenbelt, MD, X-324-73-272 (1973).

3. A. F. Emery, "Instruction Manual for the Program SHAPEFACTOR", Sandia National Laboratories, Livermore, Ca., SAND80-8027 (1980).

4. G. P. Mitalas and D. G. Stephenson, "FORTRAN IV Programs to Calculate Radiant Interchange Factors", National Research Council of Canada, Division of Building Research, Ottawa, Canada, DBR-25 (1966).

5. E. M. Sparrow and R. D. Cess, Radiation Heat Transfer, McGraw Hill, New York (1978).

6. CRAY-1 Computer System CFT Reference Manual, Cray Research Incorporated, Bloomington, MN, publication No. 2240009 (1978).

DISCLAIMER